Characterization of GaAs APDs featuring separated absorption and GaAs/AlGaAs superlattices multiplication layers using soft X-rays

Matija Colja [1,*], Marco Cautero [1], Ralf Hendrik Menk [2,3,4], Pierpaolo Palestri [5], Alessandra Gianoncelli [2], Matias Antonelli [3], Giorgio Biasiol [6], Simone Dal Zilio [6], Tereza Steinhartova [6], Camilla Nichetti [7], Fulvia Arfelli [3,7], Dario De Angelis [2], Francesco Driussi [5], Valentina Bonanni [2], Alessandro Pilotto [5], Gianluca Gariani [2], Sergio Carrato [1] and Giuseppe Cautero [2,3]

1) Department of Engineering and Architecture, University of Trieste, 34127 Trieste, Italy; 2) Elettra-Sincrotrone Trieste S.C.p.A., Area Science Park Basovizza, 34149 Trieste, Italy; 3) Istituto Nazionale di Fisica Nucleare, INFN Sezione di Trieste, 34127 Trieste, Italy; 4) Department of Medical Imaging, University of Saskatchewan, Saskatoon SK S7N 5A2, Canada; 5) Polytechnic Department of Engineering and Architecture, University of Udine, 33100 Udine, Italy; 6) IOM CNR, Laboratorio TASC, Area Science Park Basovizza, 34149 Trieste, Italy; 7) Department of Physics, University of Trieste, 34127 Trieste, Italy;

GaAs SAM-APDs

Avalanche Photo Diodes (APDs) are extremely efficient and sensitive since they are able to exploit avalanche multiplication of the photogenerated carriers: by amplifying the photocurrent above the noise floor of the read-out circuit they can dramatically improve the signal-to-noise ratio (SNR). This prerogative makes them very effective in sensing extremely weak signals, but, on the other hand, it also represents a major critical point: in fact, the multiplication is only convenient if it is possible to keep very low the noise induced by the multiplicative process.

In particular, compound semiconductors based on III-V elements like gallium arsenide (GaAs) have unique properties, such as high effective atomic number, a direct bandgap, high electric-breakdown fields and a high electron mobility. For example, due to their high Z, they possess inherent advantages, compared to Si photon counters, such as shorter absorption length for high energy x-rays. Also, thanks to their larger electronic mobility, they have shorter response times.

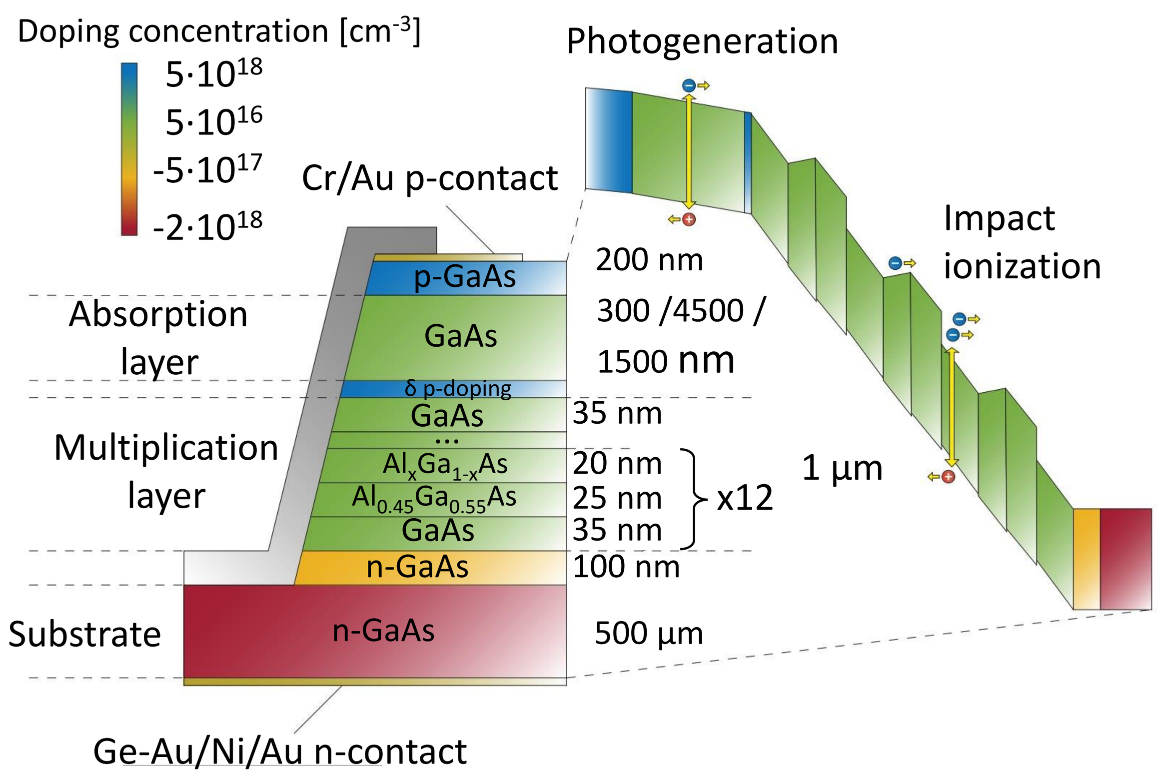

Moreover, utilizing a super-lattice structure, consisting of nanometer-sized and alternating layers of such compound semiconductors, the noise associated with charge multiplication is minimized. While their photon response and the successive charge transport can be simulated, it is essential for their fine-tuning to verify the obtained results experimentally.

FABRICATION & SIMULATIONS

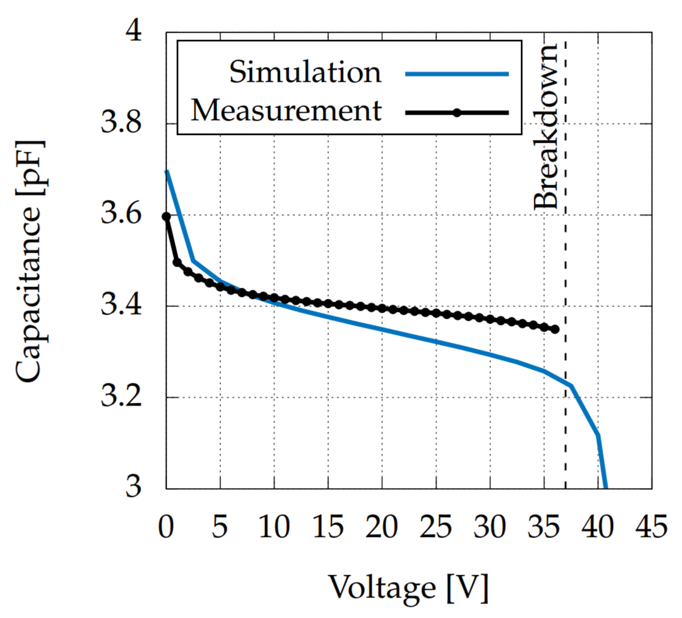

Several GaAS APDs have been grown by molecular beam epitaxy (MBE) on a 500-µm-thick heavily Si-doped n-type substrate.

Different absorption region thicknesses
- 4.5 µm
- 300 nm
- 15 µm

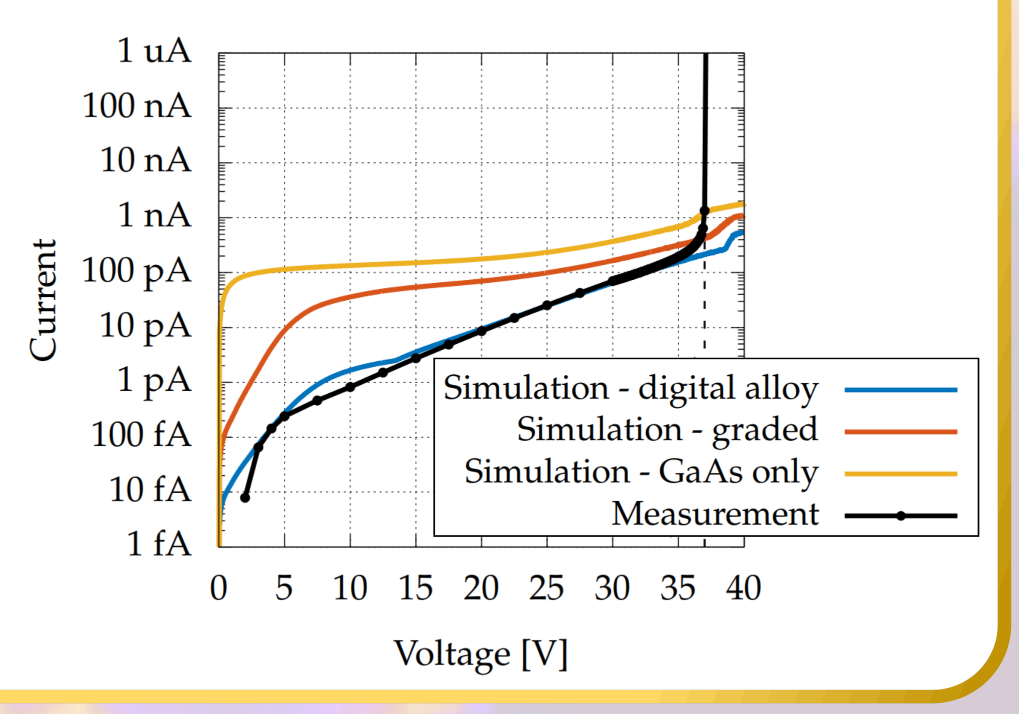

Simulations of a vertical cross section using Sentaurus TCAD Different Idark values are obtained assuming no hetero-junction as opposed to graded or digital alloy. This is a limitation of the SRH model in TCAD. CV curves instead are reproduced.

MEASUREMENTS

Laser measurements gave an estimation of the excess noise factor (ENF) and a measurement of the multiplication.

- Single hole-electron pair production due to low photon energy
- No photon penetration inside the multiplication region

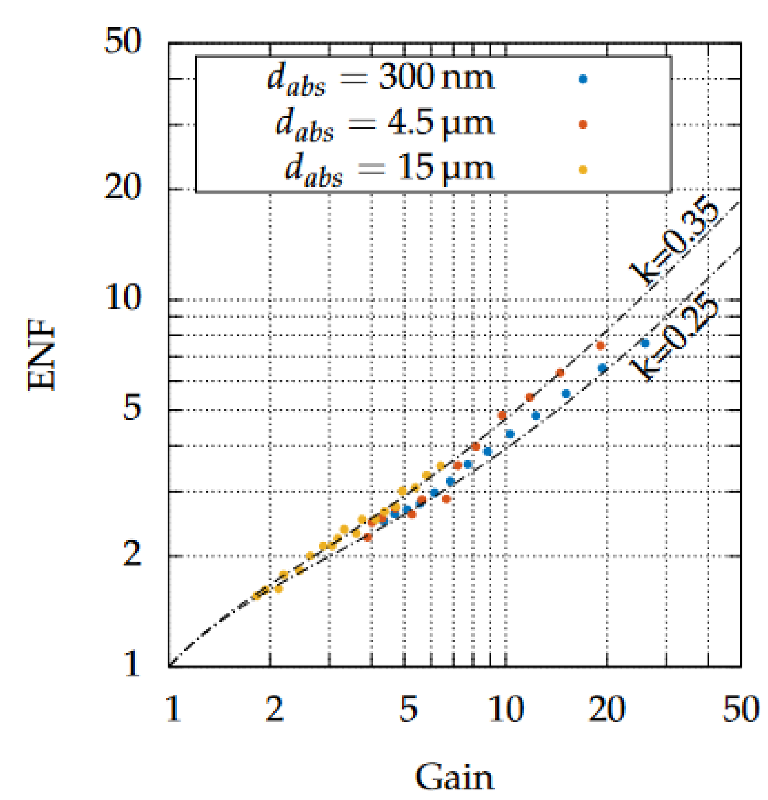

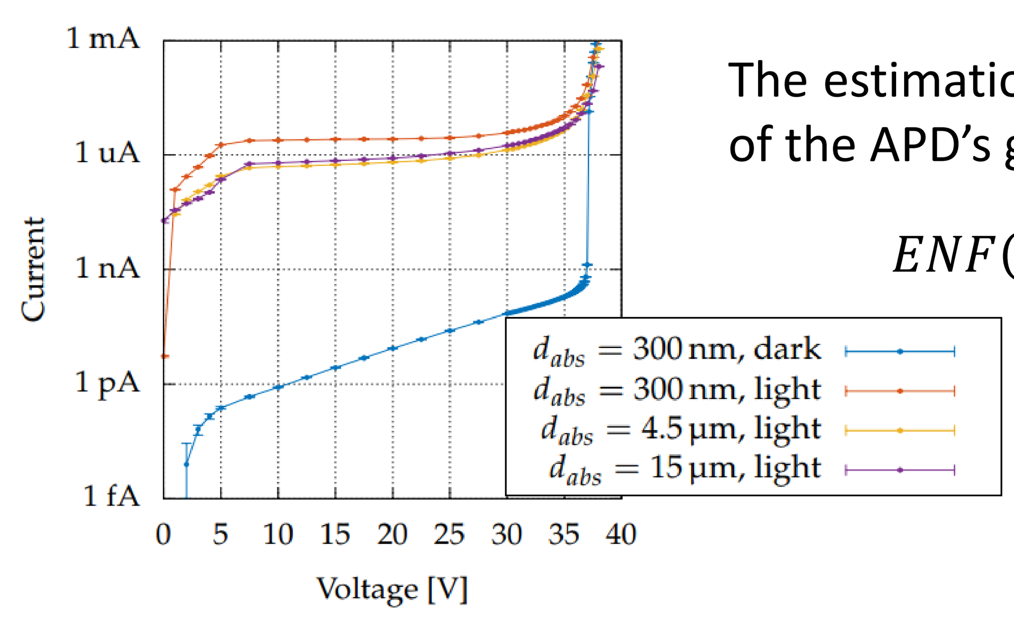

The estimation required an accurate knowledge of the APD's gain M and power spectral density.

$$ENF(M) = k \cdot M + (1-k)\left(2 - \frac{1}{M}\right)$$

$$M = \frac{I_m^{ph}(V) - I_m^{dark}(V)}{a \cdot e^{b \cdot V}}$$

SYNCHROTRON RADIATION MEASUREMENTS

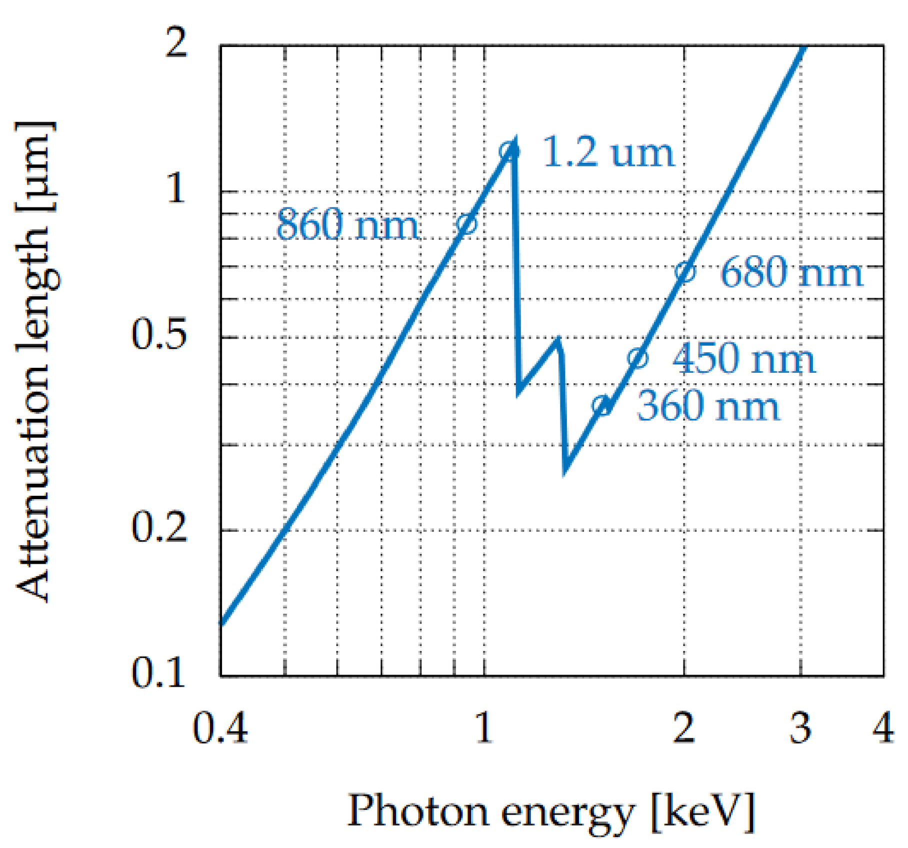

Different energies were used to have different attenuation lengths, thus producing carriers at different distances from the multiplication layer.

For each device and energy, photoinduced-current maps and X-ray fluorescence maps were taken to evaluate the device composition.

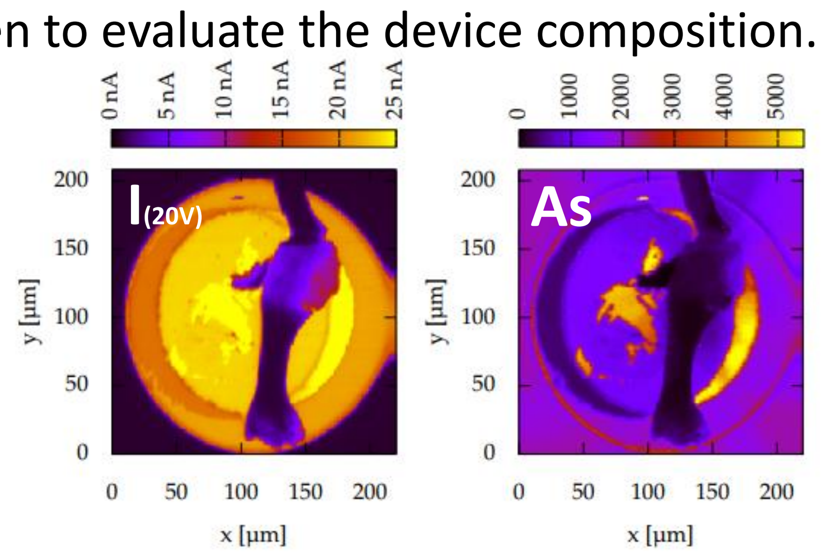

d_{abs} [µm]	Energy [eV]	Flux [10^{10} photons/s]	I_m^{GaAs} [nA]	I_{th} [nA]	η [%]
15	940	1.60	195.530 ± 0.025	573 ± 29	34.1 ± 1.7
	1090	1.95	259.754 ± 0.025	810 ± 40	32.1 ± 1.6
	1500	3.30	634.934 ± 0.025	1890 ± 94	33.7 ± 1.7
	1705	2.37	449.844 ± 0.025	1539 ± 77	29.2 ± 1.5
	2010	1.53	430.337 ± 0.025	1172 ± 59	36.7 ± 1.8
4.5	940	1.50	119.793 ± 0.025	537 ± 27	22.3 ± 1.1
	1090	1.35	125.670 ± 0.025	561 ± 28	22.4 ± 1.1
	1500	2.55	318.681 ± 0.025	1457 ± 73	21.9 ± 1.1
	1705	2.43	378.027 ± 0.025	1578 ± 79	24.0 ± 1.2
	2010	1.53	322.070 ± 0.025	1172 ± 59	27.5 ± 1.4
0.3	940	1.95	493.285 ± 0.025	698 ± 35	72.5 ± 7.9
	1500	0.69	337.861 ± 0.025	394 ± 20	83.4 ± 5.8

The acquired data substantially highlight:
- Absence of traps in the interfacial regions
- Independence of the efficiency from the thickness of the absorption region, up to 15 µm
- Devices designed not to reach the punch-through anyhow exhibit quite high photocurrents

[1] Cai, Q. et al., AlGaN Ultraviolet Avalanche Photodiodes Based on a Triple-Mesa Structure. Applied Physics Letters 2018, 113, 123503. doi:10.1063/1.5049621.
[2] Lauter, J., et al. "AlGaAs/GaAs SAM-avalanche photodiode: an X-ray detector for low energy photons." Nuclear Instruments and Methods in Physics Research Section A: Accelerators, Spectrometers, Detectors and Associated Equipment 356.2-3 (1995): 324-329.
[3] Nichetti, C. Development of Avalanche Photodiodes with Engineered Bandgap Based upon III-V Semiconductors. Unpublished doctoral thesis, University of Trieste, 2020.

*CONTACT
matija.colja@elettra.eu